

Electrophysiological properties of two axonal sodium channels, Na_v1.2 and Na_v1.6, expressed in mouse spinal sensory neurones

Anthony M. Rush^{1,2,3}, Sulayman D. Dib-Hajj^{1,2,3} and Stephen G. Waxman^{1,2,3}

¹Department of Neurology and ²Center for Neuroscience and Regeneration Research, Yale School of Medicine, New Haven, CT 06510 and ³Rehabilitation Research Center, VA Connecticut Healthcare System, West Haven, CT 06516, USA

Sodium channels Na_v1.2 and Na_v1.6 are both normally expressed along premyelinated and myelinated axons at different stages of maturation and are also expressed in a subset of demyelinated axons, where coexpression of Na_v1.6 together with the Na⁺/Ca²⁺ exchanger is associated with axonal injury. It has been difficult to distinguish the currents produced by Na_v1.2 and Na_v1.6 in native neurones, and previous studies have not compared these channels within neuronal expression systems. In this study, we have characterized and directly compared Na_v1.2 and Na_v1.6 in a mammalian neuronal cell background and demonstrate differences in their properties that may affect neuronal behaviour. The Na_v1.2 channel displays more depolarized activation and availability properties that may permit conduction of action potentials, even with depolarization. However, Na_v1.2 channels show a greater accumulation of inactivation at higher frequencies of stimulation (20–100 Hz) than Na_v1.6 and thus are likely to generate lower frequencies of firing. Na_v1.6 channels produce a larger persistent current that may play a role in triggering reverse Na⁺/Ca²⁺ exchange, which can injure demyelinated axons where Na_v1.6 and the Na⁺/Ca²⁺ exchanger are colocalized, while selective expression of Na_v1.2 may support action potential electrogenesis, at least at lower frequencies, while producing a smaller persistent current.

(Resubmitted 11 January 2005; accepted after revision 7 March 2005; first published online 10 March 2005)

Corresponding author S. G. Waxman: Department of Neurology, Yale School of Medicine, LCI 707, 333 Cedar Street, New Haven, CT 06510, USA. Email: stephen.waxman@yale.edu

Voltage-gated sodium channels are critical for electrogenesis in excitable cells; at least nine distinct sodium channel isoforms have been identified in mammals (Goldin *et al.* 2000). It is possible to study the physiological properties of these channels in isolation in cell lines or in oocytes, but the appropriate ensemble of associated proteins, such as β -subunits (Isom *et al.* 1994) may not be present, and thus it is not clear whether the characteristics recorded in these expression systems accurately reflect the *in vivo* properties of the channels.

In this study, we have characterized and compared sodium channels Na_v1.2 and Na_v1.6 in a mammalian, neuronal cell background using the technique (Cummins *et al.* 2001; Herzog *et al.* 2003) of expressing TTX-resistant (TTX-R) versions of these channels in dorsal root ganglia (DRG) neurones from Na_v1.8-null mice (Akopian *et al.* 1999), which permits recording in isolation from other sodium currents. Our rationale for comparing these two channels arises from their sequential expression during development of myelinated axons and their altered patterns of expression in demyelinated axons

under pathological conditions. Na_v1.2 is present in premyelinated CNS neurones and at immature nodes of Ranvier, before a transition to expression of Na_v1.6 at mature nodes (Boiko *et al.* 2001; Kaplan *et al.* 2001), but to date, the question of whether expression of Na_v1.6, rather than Na_v1.2, might be functionally advantageous has not been explored.

The comparative physiology of Na_v1.2 and Na_v1.6 may also be relevant to demyelinated axons. Both Na_v1.2 and Na_v1.6 are expressed along demyelinated axons in white matter from mice with experimental autoimmune encephalomyelitis (EAE) (Craner *et al.* 2003, 2004a) and in human white matter from acute multiple sclerosis (MS) plaques (Craner *et al.* 2004b). Na_v1.6, which has been shown to produce persistent current (Smith *et al.* 1998; Burbidge *et al.* 2002), is colocalized with the Na⁺/Ca²⁺ exchanger in injured axons, while Na_v1.2 is expressed, often together with the Na⁺/Ca²⁺ exchanger, along demyelinated axons that do not show signs of injury in EAE (Craner *et al.* 2004a) and in MS (Craner *et al.* 2004b), consistent with the suggestion that a persistent

sodium conductance can drive reverse $\text{Na}^+/\text{Ca}^{2+}$ exchange that contributes to axonal degeneration (Stys *et al.* 1992; Stys *et al.* 1993). Because dysmyelinated axons that express $\text{Na}_v1.2$ are much less susceptible to this type of injury (Waxman *et al.* 1990), we hypothesized that $\text{Na}_v1.2$ would produce a smaller persistent current than $\text{Na}_v1.6$.

In our comparison of $\text{Na}_v1.2$ and $\text{Na}_v1.6$, we have also examined resurgent current, which was initially recorded from Purkinje neurones and linked to the presence of $\text{Na}_v1.6$ (Raman & Bean, 1997). The resurgent current is a transient current that displays slow activation and inactivation upon rapid repolarization. Because more recent studies have led to the suggestion that other (but unspecified) sodium channel isoforms may also be able to produce resurgent current (Afshari *et al.* 2004; Do & Bean, 2004; Grieco & Raman, 2004), we compared the ability of $\text{Na}_v1.2$ and $\text{Na}_v1.6$ to produce resurgent current.

Methods

Culture of DRG neurones

We expressed and then recorded current from $\text{Na}_v1.2$ and $\text{Na}_v1.6$ channels within small DRG neurones, in which both of these channels are normally expressed (Boiko *et al.* 2001; Black *et al.* 2002). DRG neurones were cultured from mice following a protocol approved by the Yale Animal Care and Use Committee. Male mice in the age range 3–6 weeks were used (weight ~ 15 – 20 g) and were rendered unconscious by exposure to CO_2 and decapitated. DRG neurones were cultured as previously described (Caffrey *et al.* 1992). Briefly, the L4 and L5 DRGs were harvested from $\text{Na}_v1.8$ -null mice (Akopian *et al.* 1999). The DRGs were treated with collagenase A (1 mg ml^{-1}) for 25 min, and collagenase D (1 mg ml^{-1}) (Roche, Indianapolis, IN, USA) and papain ($30 \mu \text{ ml}^{-1}$) (Worthington, Lakewood, NJ, USA) for 25 min, dissociated in Dulbecco's modified Eagle's medium and Ham's F12 medium supplemented with 10% fetal bovine serum, and plated on glass coverslips.

Construction of mammalian expression vectors encoding $\text{Na}_v1.2$ and $\text{Na}_v1.6$

The cDNA construct for the expression of the TTX-R version of $\text{Na}_v1.6$ ($\text{Na}_v1.6_R$) was previously described (Herzog *et al.* 2003). Briefly, a mouse $\text{Na}_v1.6$ cDNA was inserted into a mammalian expression vector, pcDNA3.1, which was modified to render it low copy number (Klugbauer *et al.* 1995). Tyrosine 371 of the open reading frame was changed to serine (Y371S) to convert the channel into a TTX-R phenotype. The construct of rat $\text{Na}_v1.2$ in the mammalian expression vector pRC-CMV, which was a generous gift from Dr A. Goldin (University of California, Irvine), has been

previously described (Kearney *et al.* 2001). This construct was modified for the experiments reported in this study. Briefly, phenylalanine 385 of the open reading frame was changed to serine (F385S) to convert the channel into a TTX-R phenotype ($\text{Na}_v1.2_R$), and the FLAG epitope (DYKDDDDK), which was engineered at the N-terminus of the channel, was deleted to restore the wild-type sequence. The two modifications were introduced sequentially with two pairs of mutagenic primers using the QuickChange XL mutagenesis kit (Stratagene, La Jolla, CA, USA). The entire cDNA insert was sequenced at the Howard Hughes Medical Institute/Keck Biotechnology Center at Yale University. Sequence comparison with the parent plasmid did not show any additional, unintended changes in the sequence of the open reading frame.

Biolistic transfection of $\text{Na}_v1.8$ -null DRG neurones

The Helios Gene Gun System (Bio-Rad Laboratories) was used for biolistic transfection of neurones (Wellmann *et al.* 1999), after 5–6 days in culture. $\text{Na}_v1.2_R$ or $\text{Na}_v1.6_R$ DNA ($10 \mu \text{g}$) was mixed with $5 \mu \text{g}$ green fluorescent protein (GFP) DNA, and biolistic cartridges were made as previously described (Cummins *et al.* 2001) using $1.6 \mu \text{m}$ gold particles. Immediately prior to biolistic transfection, the culture medium was removed from the well; the gene gun was held ~ 2 cm above the cells and a pressure of ~ 120 p.s.i. (~ 827 kPa) was used to discharge the gold particles. Electrophysiological studies were carried out 18–48 h after transfection, and the majority of cells that expressed GFP also expressed fast TTX-R sodium currents. In previous studies (Cummins *et al.* 2001; Herzog *et al.* 2003), these currents were not observed in either untransfected cells or cells transfected with only GFP, confirming that the TTX-R currents we recorded were specific to the recombinant $\text{Na}_v1.2_R$ or $\text{Na}_v1.6_R$. Moreover, the maximal contamination by $\text{Na}_v1.9$ currents is ≤ 300 pA with transfection of GFP alone when a holding potential of -120 mV is used (Cummins *et al.* 2001).

Electrophysiology

Standard whole-cell voltage-clamp recordings were made from small-diameter DRG neurones using an Axopatch 200B amplifier (Axon Instruments, Union City, CA, USA). These cells were chosen based on their distinctive rounded cell body morphology, in contrast to any glial cells in the cultures. In order to selectively record sodium currents, the pipette solution contained (mM) 140 CsF, 1 EGTA, 10 NaCl and 10 Hepes; pH 7.3; adjusted to $310 \text{ mosmol l}^{-1}$ with glucose. The external solution contained (mM): 140 NaCl, 3 KCl, 1 MgCl_2 , 1 CaCl_2 , 20 TEACl, 5 CsCl, 0.1 CdCl_2 , 10 Hepes; pH 7.3; adjusted to $320 \text{ mosmol l}^{-1}$ with glucose (all Sigma, St Louis, MO, USA). For isolation of

the TTX-R $\text{Na}_v1.2_R$ or $\text{Na}_v1.6_R$ currents, $0.25 \mu\text{M}$ TTX was added to the external solution. The pipette potential was zeroed before seal formation and the voltages were not corrected for liquid junction potential. Capacity transients were cancelled and series resistance (of $\sim 1\text{--}3 \text{ M}\Omega$) was compensated by 85–90%. Leakage current was digitally subtracted online using hyperpolarizing potentials applied after the test pulse (P/6 procedure). Similar results could be obtained when using depolarizing leakage currents. Currents were acquired using Clampex 8.1 software, filtered at 5 kHz and at a sampling rate of 20–50 kHz, via a Digidata 1200 series interface (Axon Instruments). Cell capacitance was not statistically different between groups of the cells studied electrophysiologically ($P > 0.05$). All experiments were performed at room temperature ($21\text{--}25^\circ\text{C}$). Data are expressed as mean \pm s.e.m. and statistical analyses were performed using Student's t test (significance at least $P < 0.05$), where we assume the apparent Gaussian nature of the data sets would be extended to the population. Any cells that were not well voltage clamped (as judged by sudden changes in recorded current, with small changes in depolarization) were discarded and excluded from the analysis.

Voltage protocols were as follows. Standard current–voltage ($I\text{--}V$) families were obtained using 40 ms pulses from a holding potential of -100 mV , to a range of potentials (-65 mV to $+60 \text{ mV}$) every 5 s. The peak value at each potential was plotted to form $I\text{--}V$ curves. Activation curves were fitted with the following Boltzmann distribution equation:

$$G_{\text{Na}} = G_{\text{Na,max}} / (1 + \exp((V_{1/2} - V_m)/k)) \quad (1)$$

where G_{Na} is the voltage-dependent sodium conductance, $G_{\text{Na,max}}$ is the maximal sodium conductance, $V_{1/2}$ is the potential at which activation is half maximal, V_m is the membrane potential and k is the slope. A theoretical reversal potential of 69.9 mV was used in calculations, whereas the measured potentials were $\sim 60 \text{ mV}$, probably due to the difficulty of completely blocking outward potassium currents in these cells. Availability protocols consisted of a series of prepulses (-140 mV to 10 mV) lasting 500 ms, from the holding potential of -100 mV , followed by a 40 ms depolarization to -10 mV , every 10 s. The normalized curves were fitted using a Boltzmann distribution equation:

$$I_{\text{Na}}/I_{\text{Na,max}} = 1 / (1 + \exp((V_m - V_{1/2})/k)) \quad (2)$$

where $I_{\text{Na,max}}$ is the peak sodium current elicited after the most hyperpolarized prepulse, V_m is the preconditioning pulse potential, $V_{1/2}$ is the half-maximal sodium current and k is the slope factor. For recovery from inactivation experiments, two 40 ms stimuli were given to the voltage that previously produced peak current from the holding potential of -100 mV , with a variable recovery time period

in the range of 0.1 ms to 200 ms. Curves were fitted with a single rising exponential function.

Results

Expression of $\text{Na}_v1.2_R$ and $\text{Na}_v1.6_R$ in DRG neurones

To study the properties of isolated $\text{Na}_v1.2$ or $\text{Na}_v1.6$ sodium currents in a mammalian neuronal cell background, we expressed TTX-R versions of these channels (termed $\text{Na}_v1.2_R$ and $\text{Na}_v1.6_R$ in this paper), made by replacing the appropriate phenylalanine ($\text{Na}_v1.2$) or tyrosine ($\text{Na}_v1.6$) at the TTX binding site with a serine (Cummins *et al.* 2001; Herzog *et al.* 2003), in DRG neurones from $\text{Na}_v1.8$ -null mice, which lack expression of functional, slow TTX-R $\text{Na}_v1.8$ currents (Akopian *et al.* 1999) and show extremely low levels ($< 300 \text{ pA}$) of the persistent TTX-R $\text{Na}_v1.9$ currents after several days in culture (Cummins *et al.* 2001). In these cells, when endogenous, fast TTX-S channels are blocked with TTX, the recombinant channels can be electrophysiologically characterized in isolation (Cummins *et al.* 2001; Herzog *et al.* 2003). $\text{Na}_v1.8$ -null DRG neurones were biolistically transfected with either $\text{Na}_v1.2_R$ or $\text{Na}_v1.6_R$, together with GFP, to identify transfected neurones. Recordings were performed 18–48 h later, giving ample time for robust expression of the channels. Previously, transfection with GFP alone was shown to produce no TTX-R currents (Herzog *et al.* 2003).

Figure 1 shows families of currents from DRG neurones transfected with $\text{Na}_v1.2_R$ (A) and $\text{Na}_v1.6_R$ (B) elicited using a series of depolarizations from a holding potential of -100 mV (inset). This protocol produced robust fast-activating and fast-inactivating sodium currents. The average peak current was $7.8 \pm 1.8 \text{ nA}$ ($n = 25$) for cells transfected with $\text{Na}_v1.2_R$ and $15.1 \pm 2.8 \text{ nA}$ ($n = 27$) for cells transfected with $\text{Na}_v1.6_R$.

Figure 1C shows the current–voltage relationship for the two recombinant channels and Fig. 1D shows the activation and availability curves. Availability experiments were performed from a holding potential of -100 mV , using 500 ms prepulses to a range of potentials (-100 to 0 mV), before a test depolarization to -10 mV . DRG neurones expressing $\text{Na}_v1.6_R$ displayed activation and availability values that were significantly hyperpolarized from those in neurones expressing $\text{Na}_v1.2_R$. The midpoints of activation were $-24.4 \pm 1.5 \text{ mV}$ ($n = 23$) for $\text{Na}_v1.2_R$, compared to $-35.9 \pm 1.5 \text{ mV}$ ($n = 24$) for $\text{Na}_v1.6_R$, and midpoints of availability were $-56.6 \pm 1.9 \text{ mV}$ ($n = 10$) for $\text{Na}_v1.2_R$, compared to $-70.6 \pm 1.6 \text{ mV}$ ($n = 11$) for $\text{Na}_v1.6_R$. It should be noted that it is possible that the 500 ms prepulses used for the availability curves induced some slow inactivation (see Fig. 4). We further characterized the currents by fitting the inactivation portion of the transient current with a double exponential

function. Time constants derived from these data are shown in Fig. 1E and F ($n = 6-7$). There were no significant differences in the fitted parameters between the two channels.

Persistent current

Previous studies have shown that $\text{Na}_v1.6$ can produce a persistent or non-inactivating current (Smith *et al.* 1998;

Burbidge *et al.* 2002) and that $\text{Na}_v1.2$ may produce a persistent current when coexpressed with G-protein $\beta\gamma$ subunits (Ma *et al.* 1997), but have not addressed whether there would be more persistent current with $\text{Na}_v1.6$ expression *versus* $\text{Na}_v1.2$ within a mammalian neuronal background. Figure 2 shows representative currents, on a large scale, from DRG neurones transfected with $\text{Na}_v1.2_R$ (A) and $\text{Na}_v1.6_R$ (B). Similar to the studies cited above, the amplitude of the persistent current was measured 30 ms

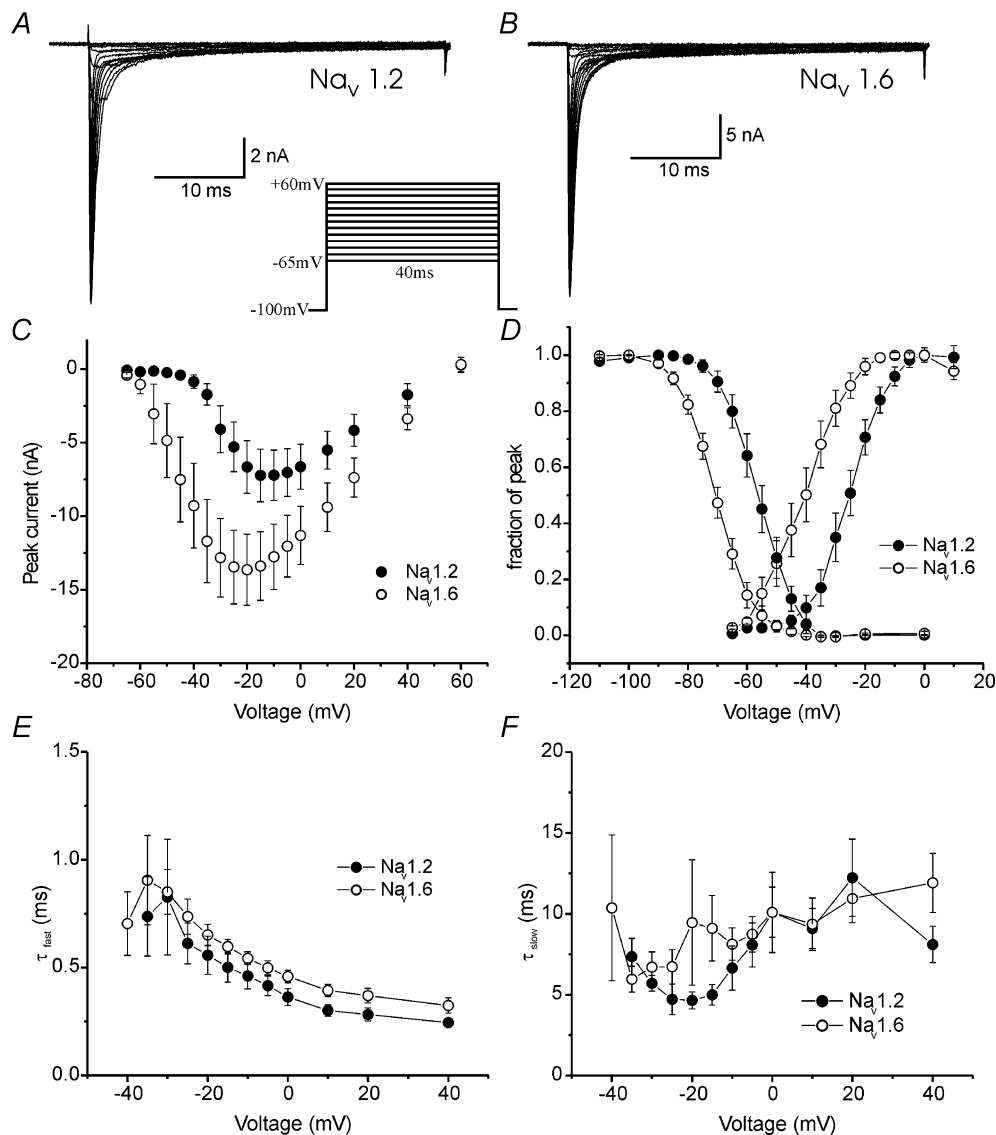


Figure 1. Comparison of $\text{Na}_v1.2_R$ and $\text{Na}_v1.6_R$ current properties

Representative families of currents recorded from $\text{Na}_v1.8$ -null DRG neurones expressing $\text{Na}_v1.2_R$ channels (A) or $\text{Na}_v1.6_R$ channels (B) are shown. Currents were elicited by 40 ms depolarizations from a holding potential of -100 mV to a range of potentials between -65 mV and $+60$ mV (inset). C, average absolute current–voltage relationship for the two channels ($\text{Na}_v1.2$, $n = 25$; $\text{Na}_v1.6$, $n = 27$). D, activation and availability curves for $\text{Na}_v1.2_R$ ($n = 23/10$) and $\text{Na}_v1.6_R$ ($n = 24/11$). Activation was calculated from current–voltage experiments, as detailed in Methods. Availability of channels was estimated by measuring the peak current amplitude elicited by 40 ms test pulses to -10 mV following 500 ms prepulses to a range of voltages from -110 mV to 0 mV. Values were normalized to peak and plotted *versus* voltage. E and F, Inactivation time constants (E, fast; F, slow) for double exponential fits of the decay phase of currents elicited at the potentials shown for 40 ms. Relative amplitudes of the fits were 60–88% for τ_{fast} and 12–40% for τ_{slow} . C–F show mean \pm S.E.M.

into the voltage step. The amplitude for each current is plotted *versus* voltage in Fig. 2C. This clearly shows that $\text{Na}_v1.6_R$ produced substantially more persistent current than $\text{Na}_v1.2_R$, across a range of voltages ($P < 0.05$ (*)). The slightly biphasic nature of the $I-V$ curve may be in part due to a minor contamination with a small remaining $\text{Na}_v1.9$ current in these cells. However, the persistent current activates over a different voltage range from that expected for $\text{Na}_v1.9$ (Cummins *et al.* 1999), and shows a significant difference with expression of the different constructs. The reversal potential is also less depolarized than would be expected for a sodium current, and this may be due to a level of unblocked outward potassium current. Despite these technical difficulties, the distinctly larger persistent current recorded with $\text{Na}_v1.6_R$ expression compared to $\text{Na}_v1.2_R$, strongly suggests that the currents recorded are due to sodium flow through the transfected channels. As noted above, transient $\text{Na}_v1.6_R$ currents were larger than $\text{Na}_v1.2_R$ currents, when expressed in DRG neurones. When the persistent currents were scaled appropriately, to take this into account, $\text{Na}_v1.6_R$ persistent current was $\sim 5\%$ of the transient current, and the $\text{Na}_v1.2_R$ persistent current was $\sim 3\%$ of the transient current, over the voltage range -60 mV to -15 mV.

Recovery from inactivation

The repriming or recovery from inactivation of TTX-S currents is fast (~ 10 ms) in large (Everill *et al.* 2001), and slow (~ 90 ms) in small (Elliott & Elliott, 1993; Cummins & Waxman, 1997) DRG neurones, and this may be due, in part, to the differential expression of sodium channel subtypes (Herzog *et al.* 2003). In this study, we directly compared the repriming kinetics of $\text{Na}_v1.2_R$ and $\text{Na}_v1.6_R$, following a single depolarizing stimulus, after expression within DRG neurones and found that recovery from inactivation was fast for both channels. Figure 3 shows representative currents for $\text{Na}_v1.2_R$ (A) and $\text{Na}_v1.6_R$ (B) using the repriming protocol shown in the inset, and a recovery voltage of -80 mV. Cells were held at -100 mV, depolarized to -10 mV for 40 ms to activate currents, then allowed to recover for increasing lengths of time (at a number of different voltages), followed by a test depolarization, to -10 mV for 40 ms, to measure the extent of recovery. This protocol was repeated for a variety of recovery voltages, from -100 to -70 mV. Figure 3C shows the time-course of repriming from -80 mV; the time constants, using a single exponential fit, are shown plotted against voltage in Fig. 3D. These data show that $\text{Na}_v1.2_R$ repriming more rapidly during the first 50 ms, after a single depolarizing stimulus, than $\text{Na}_v1.6_R$ over this voltage range ($P < 0.05$ (*)) but that the recovery for both channels is generally fast ($\sim 2-10$ ms).

Development of closed-state inactivation

In previous studies, the current produced by $\text{Na}_v1.6_R$ after expression in DRG neurones (Herzog *et al.* 2003), and TTX-S currents (produced by channels whose molecular identities have not been established) in small DRG neurones (Cummins & Waxman, 1997) were found to develop inactivation more rapidly (~ 20 ms) compared to

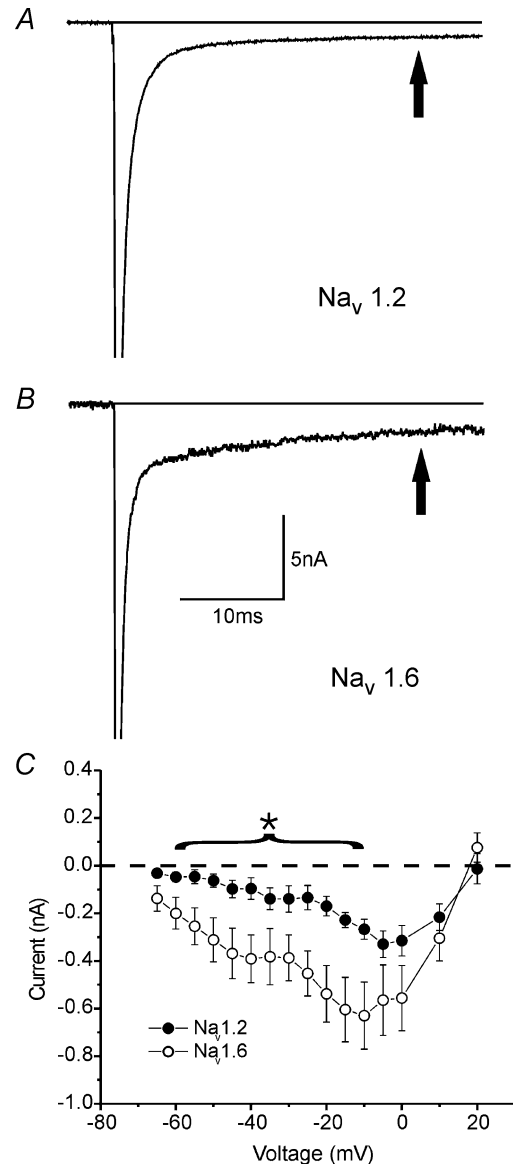


Figure 2. $\text{Na}_v1.6_R$ displays a larger persistent current than $\text{Na}_v1.2_R$ in $\text{Na}_v1.8$ -null DRG neurones

Representative currents, on an expanded scale, demonstrating the larger persistent current, in response to a -10 mV stimulus from a holding potential of -100 mV displayed by $\text{Na}_v1.6_R$ (B) ($n = 12$), compared to $\text{Na}_v1.2_R$ (A) ($n = 14$). Currents were elicited from a holding potential of -100 mV to the voltages between -65 mV and $+20$ mV for 40 ms. The amplitude of the current was measured 30 ms into the voltage step, as the arrows indicate, and plotted for a range of voltages (C). * $P < 0.05$. Scale in B refers to panels A and B. C show mean \pm s.e.m.

Na_v1.7 (~150 ms) (Cummins *et al.* 1998). To compare development of inactivation by Na_v1.2_R and Na_v1.6_R channels after expression in DRG neurones, cells were held at -100 mV, depolarized to a particular voltage (e.g. -70 mV) for increasing amounts of time and then the level of current was tested with a depolarization to -10 mV for 40 ms (Fig. 4A inset). As expected, the level of inactivation increased as the time at the depolarized voltage was extended, as shown in the representative currents for Na_v1.2_R (Fig. 4A) and Na_v1.6_R (Fig. 4B). Due to the large differences in availability of channels at these voltages (see Fig. 1D), Na_v1.2_R currents inactivated less at, for instance, -80 mV (Fig. 4C) and -60 mV (Fig. 4D) than the Na_v1.6_R currents. In order to estimate the onset of inactivation, these data were fitted with a double exponential and these values are plotted in Fig. 4E (fast time constant) and Fig. 4F (slow time constant). The time constants were consistent across the range of voltages tested (-80 to -50 mV). Na_v1.2_R displayed slower development of inactivation (~30 ms) compared to Na_v1.6_R (~10 ms) ($P < 0.02$ (*)).

Resurgent current

Resurgent current has been widely associated with the presence of Na_v1.6 (Raman & Bean, 1997; Swensen & Bean, 2003), but more recently it has been suggested that other sodium channel subtypes can also demonstrate this phenomenon (Afshari *et al.* 2004; Do & Bean, 2004; Grieco & Raman, 2004). In this study, we examined the incidence of this current with expression of Na_v1.2_R or Na_v1.6_R in DRG neurones. We used a standard protocol (Fig. 5A inset) to elicit the current, where the cells were held at -100 mV, depolarized to +30 mV for 20 ms and then repolarized to a range of potentials from -80 mV to +20 mV for 40 ms. Only those cells that demonstrated robust, clear resurgent current, i.e. currents that displayed the typical slow activation and inactivation of resurgent current upon repolarization, were included in our analysis. In two out of 25 of the cells transfected with Na_v1.2_R, a resurgent current could be clearly observed (~5% of the transient peak current). These currents measured 475 and 313 pA at -35 mV. Example currents are shown in Fig. 5A. There

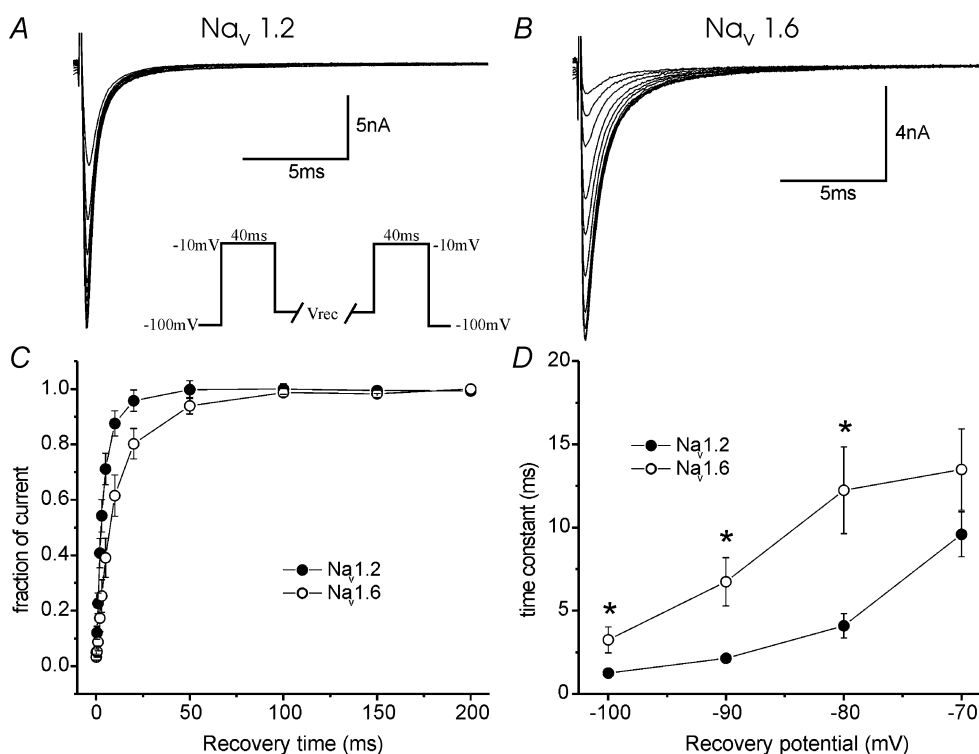
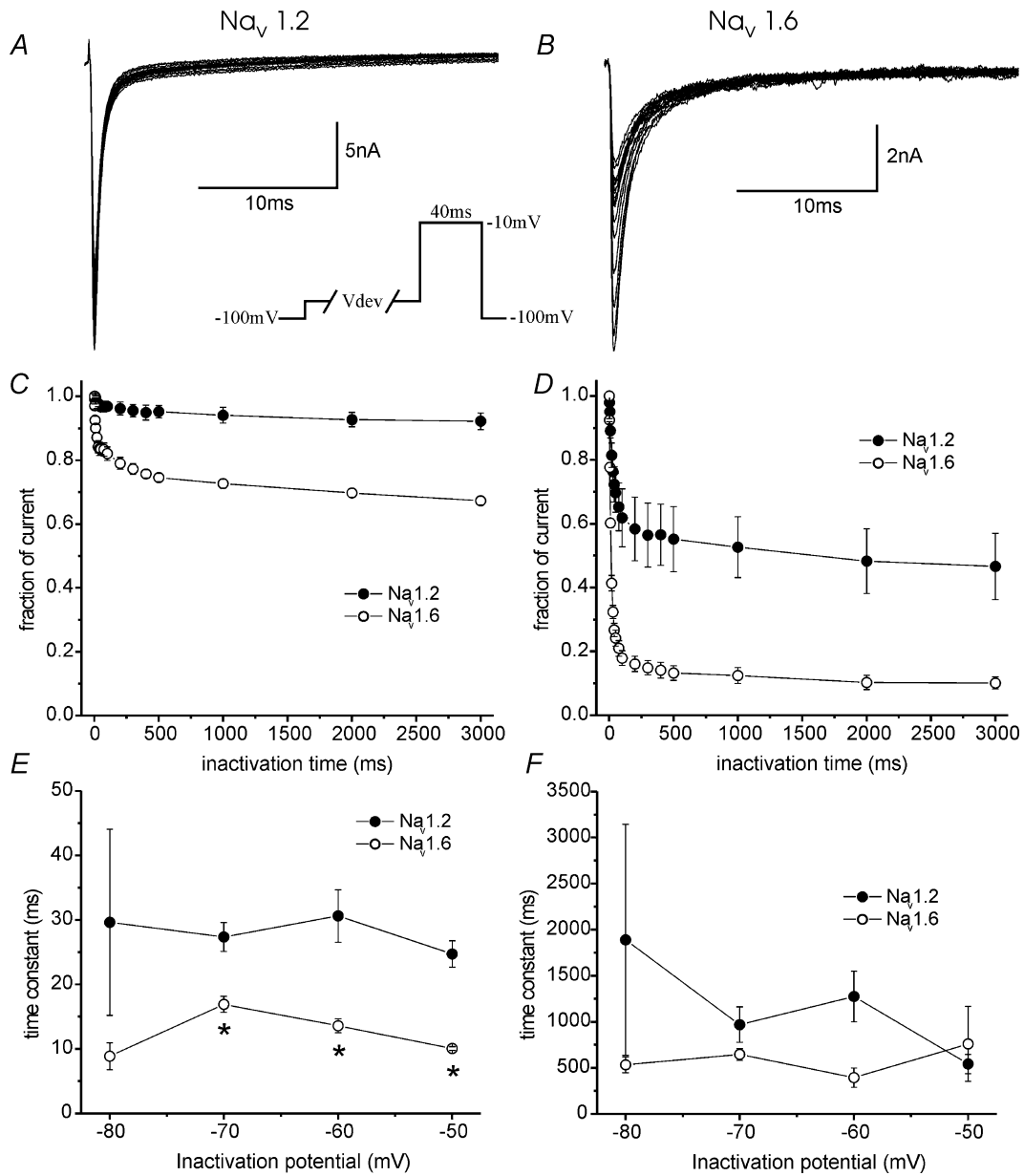


Figure 3. Repriming (recovery from inactivation) from a single depolarizing stimulus is faster for Na_v1.2_R than Na_v1.6_R channels, expressed in DRG neurones

Families of currents of DRG neurones expressing Na_v1.2_R (A) and Na_v1.6_R (B) elicited using a recovery from inactivation protocol (inset), using -80 mV as the recovery voltage (V_{rec}) voltage in these cases. For this set of experiments, cells were held at -100 mV, depolarized to -10 mV for 40 ms and then allowed to recover for increasing amounts of time, at a variety of voltages, before the test potential to -10 mV for 40 ms to measure the extent of recovery. Averaged data at a V_{rec} of -80 mV are plotted in C, demonstrating single exponential fits to the results. The fitted time constants at the range of voltages tested (-100 to -70 mV) are plotted in D, showing fast repriming for both channels and faster recovery from inactivation for Na_v1.2_R * $P < 0.05$, under these conditions ($n = 6-8$). C, D show mean \pm s.e.m.

is no evidence in the literature of a TTX-R resurgent current; in the unlikely (and unproven) event that $Na_v1.9$ is capable of producing a resurgent current, it would in the worst case display an amplitude of 5–7% (percentages taken from this study, which are not dissimilar to the previous studies of resurgent current) of 300 pA, i.e.

15–21 pA, and thus could not account for the resurgent current that we observed. The resurgent current (~7% of the transient peak current) could be found in six out of 27 (22%) cells where $Na_v1.6_R$ was expressed; representative currents are shown in Fig. 5B. Figure 5C shows a plot of average amplitudes of the resurgent current produced by



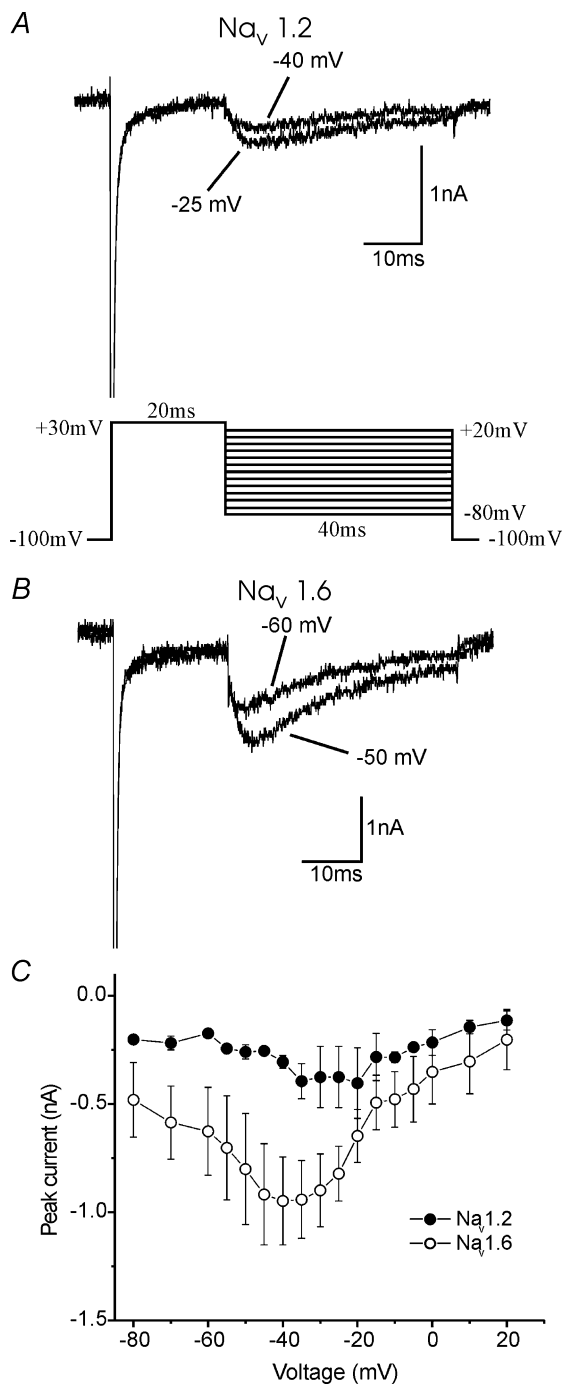


Figure 5. $\text{Na}_v1.2_R$ and $\text{Na}_v1.6_R$ can produce resurgent current in $\text{Na}_v1.8$ -null DRG neurones

Representative resurgent currents are shown for $\text{Na}_v1.2_R$ (A) and $\text{Na}_v1.6_R$ (B) after activation by a protocol (inset) where cells were held at -100 mV, depolarized to $+30$ mV for 20 ms, followed by repolarizations to a range of voltages (-80 to $+20$ mV) to elicit resurgent current. In 8% (2 out of 25) of the cells transfected with $\text{Na}_v1.2_R$, a resurgent current could be clearly observed. Resurgent current could be found in 22% (6 out of 27) of cells where $\text{Na}_v1.6_R$ was expressed. Averaged data from only those cells producing the current are shown in C. C show mean \pm S.E.M.

the two channels, although we were unable to statistically test any difference in amplitude due to the relatively low incidence of the current.

Use-dependent fall-off

Because the presence of $\text{Na}_v1.6$ current has previously been linked with rapid, burst firing (Raman *et al.* 1997; Khaliq *et al.* 2003; Swensen & Bean, 2003), we studied the ability of $\text{Na}_v1.2_R$ and $\text{Na}_v1.6_R$ to follow high-frequency stimulation, from a -80 mV holding potential. For this study, we used two main protocols consisting of either 40 ms depolarizations or 5 ms depolarizations to -10 mV, at a range of frequencies, for 20 episodes from a holding potential of -80 mV (see Fig. 6A and B; inset). Figure 6A shows examples of the first and last currents elicited in a train of 20 pulses of 40 ms at 0.5 Hz (top panels) and 20 Hz (bottom panels) for the two channels. There was very little fall-off of current with the 0.5 Hz stimulation, but at 20 Hz, there was substantial fall-off of the current beginning with the second pulse and reaching a level of $>50\%$ fall-off after 20 pulses (Fig. 6C). Figure 6B shows examples of currents elicited by 5 ms depolarizations at 0.5 Hz (top panels) and 100 Hz (bottom panels) for the two channels. The fall-off at the higher frequency stimulation of 100 Hz is clearly shown in Fig. 6D. At both 20 Hz and 100 Hz, beginning after the second pulse, there was more fall-off for $\text{Na}_v1.2_R$ than for $\text{Na}_v1.6_R$. This property was studied across a range of stimulation frequencies and these data are summarized in Fig. 6E (40 ms pulses) and Fig. 6F (5 ms pulses). The channels had nearly identical behaviour at low frequencies of stimulation, but at higher frequencies (>20 Hz), $\text{Na}_v1.6_R$ currents were able to maintain their amplitude more than the $\text{Na}_v1.2_R$ currents ($P < 0.05$ (*)). These results suggest that cells that express $\text{Na}_v1.6$ may be better high-frequency followers than cells that express $\text{Na}_v1.2$.

Discussion

This study examined the voltage-dependent and kinetic properties of two of the TTX-S sodium channels, $\text{Na}_v1.2$ and $\text{Na}_v1.6$, which are expressed along premyelinated, myelinated and demyelinated axons. Specific blockers for these channels are not available and thus it has been impossible to characterize their endogenous currents in isolation. We have been able to study the currents produced by these different channel isoforms and directly compare their properties in a mammalian, neuronal cell background. This comparison, in conditions that mimic the *in vivo* situation, provides insight into how the properties of particular channels may influence the behaviour of neurones where these channels are expressed.

In this study, the voltage-dependent properties of activation and availability of the transient sodium currents were around 15 mV more depolarized for $\text{Na}_v1.2_R$ than

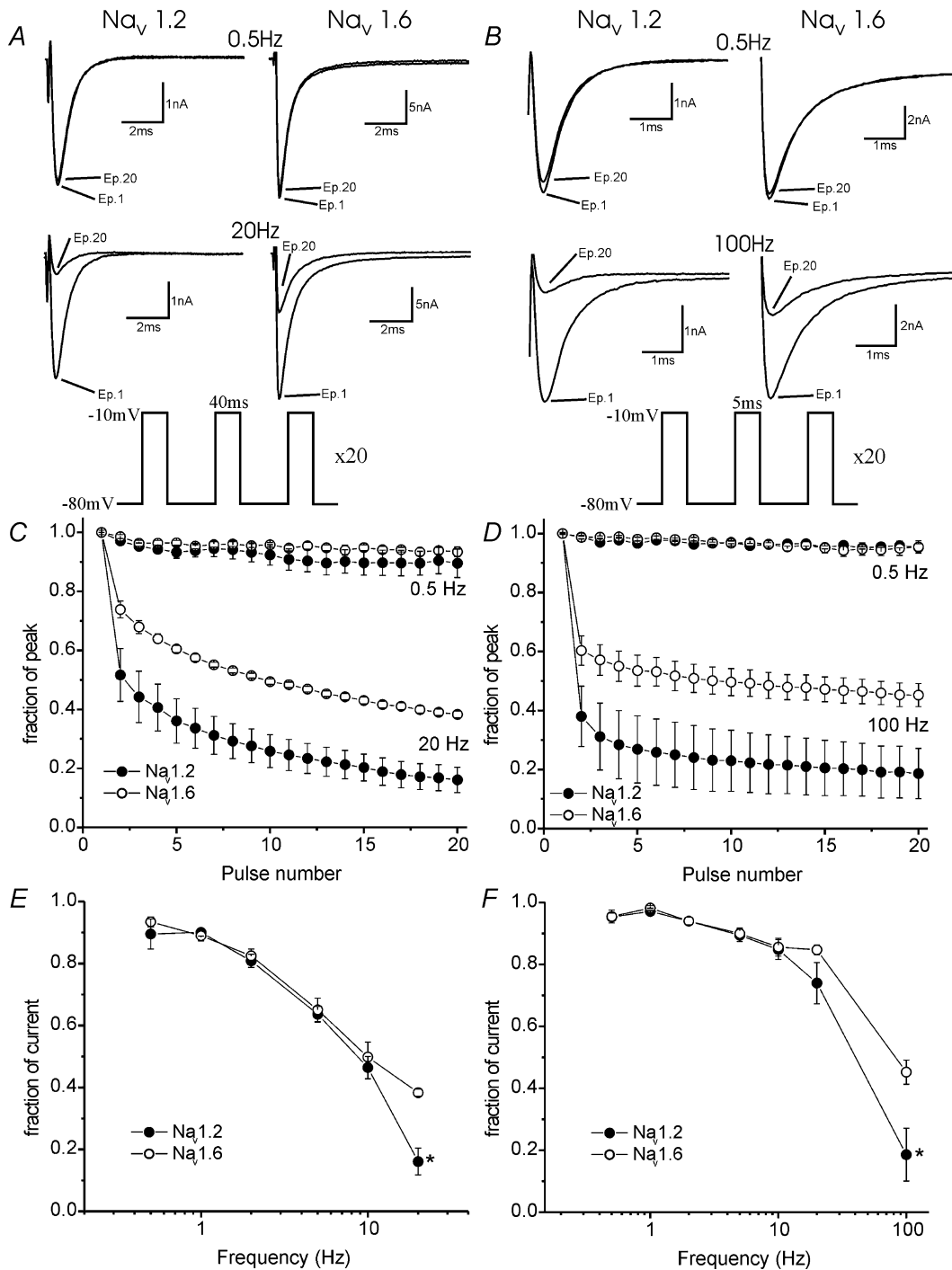


Figure 6. $Na_v1.6_R$ currents can follow high-frequency stimulation more faithfully than $Na_v1.2_R$ currents

Experiments were performed to examine the behaviour of the two currents with high-frequency stimulation using two protocols (both insets). Cells were held at -80 mV and depolarized to -10 mV for 40 ms for 20 episodes at a variety of frequencies. (A) Representative first and last currents from such a train are shown at 0.5 Hz (top panels) or 20 Hz (bottom panels). Averaged data are summarized in C. B, representative first and last currents from a train using 5 ms episodes are shown at 0.5 Hz (top panels) or 100 Hz (bottom panels). Averaged data are summarized in D. These experiments were performed at a range of frequencies (0.5–20/100 Hz) and the fraction of current remaining over the 20 episodes is plotted versus frequency for 40 ms episodes (E) and for 5 ms episodes (F) ($n = 6-11$). $Na_v1.6_R$ currents were able to maintain their amplitude more than $Na_v1.2_R$ currents ($*P < 0.05$), suggesting that cells that express $Na_v1.6$ may be better high-frequency followers than cells that express $Na_v1.2$. C–F show mean \pm S.E.M.

Na_v1.6_R. This is consistent with results from previous studies in which Na_v1.2 and Na_v1.6 were expressed in mammalian cell lines though under non-identical conditions, which taken together suggest that Na_v1.6 activates and inactivates at more hyperpolarized potentials than Na_v1.2 (Xie *et al.* 2001; Burbidge *et al.* 2002). As with a previous study from our group of sodium channel physiology, which compared Na_v1.6 and Na_v1.7 (Herzog *et al.* 2003), the parallel shift of activation and availability curves for Na_v1.2 *versus* Na_v1.6 currents is consistent with the hypothesis (Chahine *et al.* 1994) that activation and inactivation are linked. More robust expression of Na_v1.2, which occurs in some demyelinated axons (Craner *et al.* 2003, 2004a,b), could endow a neuronal membrane with the capability to fire action potentials from resting membrane potentials that are much more depolarized than normal. With tissue damage, the external potassium concentration may rise; this could depolarize neurones and the expression of Na_v1.2 could help maintain firing in such a situation, although the change in resting membrane potential (if any) in demyelinated axons compared to normal axons is not known. However, if both isoforms were present, the combination of channels could provide a cross-over current and make the axon unstable, which might explain why Na_v1.2 has to be completely replaced by Na_v1.6 at nodes of Ranvier along normal myelinated axons (Boiko *et al.* 2001; Kaplan *et al.* 2001).

It has been suggested that Na_v1.6 produces a large persistent current (Smith *et al.* 1998; Burbidge *et al.* 2002), but no direct comparison with other sodium channel isoforms has been carried out. In our experiments, both Na_v1.2_R and Na_v1.6_R produced a significant persistent current but the Na_v1.6_R current was two-fold larger. Consistent with production of a robust persistent current by Na_v1.6, a large, TTX-S persistent sodium current is present within DRG neurones (Baker & Bostock, 1997), which express Na_v1.6 at high levels (Black *et al.* 1996). Na_v1.6 is coexpressed with the Na⁺/Ca²⁺ exchanger (NCX) in injured axons while Na_v1.2 and the NCX tended to be expressed along axons that did not show signs of injury in mice with EAE (Craner *et al.* 2004a) and in human MS tissue (Craner *et al.* 2004b). Persistently activated sodium channels have been proposed to drive an injury cascade via reverse Na⁺/Ca²⁺ exchange (Stys *et al.* 1992, 1993). Conversely, dysmyelinated axons, which express Na_v1.2 (Westenbroek *et al.* 1989; Boiko *et al.* 2001), have been shown to be much less susceptible to injury triggered by sodium channels (Waxman *et al.* 1990). The results of the present study support the notion that expression of Na_v1.6, which occurs in some demyelinated axons in EAE (Craner *et al.* 2003, 2004a) and in MS (Craner *et al.* 2004b), could lead to a larger persistent current than with the other sodium channel isoform expressed along demyelinated axons (Na_v1.2), and could initiate a damaging flux of ions, contributing to axonal degeneration.

Endogenously expressed TTX-S and TTX-R sodium channels in DRG neurones produce currents with very different repriming or recovery from inactivation (Elliott & Elliott, 1993; Rush *et al.* 1998). Different TTX-S currents can also show distinct repriming characteristics following a single depolarizing stimulus, where those in small DRG neurones have slow recovery from inactivation and those in large neurones, fast (Cummins & Waxman, 1997; Everill *et al.* 2001). This may be due to differential expression of Na_v1.7 and Na_v1.6 in these neurones (Herzog *et al.* 2003), endowing these neurones with slow and fast repriming, respectively. Consistent with previous studies from both a cell line and neurones (Burbidge *et al.* 2002; Herzog *et al.* 2003), we confirm that repriming of Na_v1.6_R after a single depolarizing stimulus is fast. Previous work on Na_v1.2 in an HEK293 cell line reported recovery from inactivation that was around three times slower than that for Na_v1.6 (O'Leary, 1998). In contrast to this, in our direct comparison within a mammalian neuronal background, we found that repriming during the first 50 ms following a single depolarizing stimulus was more rapid for the Na_v1.2_R isoform. Although this result may seem surprising given that Na_v1.6 has been linked with rapid, burst firing (Raman *et al.* 1997; Swensen & Bean, 2003), we found that Na_v1.6 was able to more faithfully follow high-frequency repetitive stimuli, a characteristic described below.

Slow development of inactivation, which characterizes Na_v1.7 (Cummins *et al.* 1998; Herzog *et al.* 2003) and Na_v1.3 (Cummins *et al.* 2001) channels, is associated with more robust responses to slow depolarizing inputs (Cummins *et al.* 1998). In contrast, Na_v1.6 displays relatively rapid onset of inactivation (Herzog *et al.* 2003), and this was confirmed in the present study. Na_v1.2_R showed slightly slower onset (time constants of ~30 ms instead of ~10 ms), but this was still very much quicker than for Na_v1.3 and Na_v1.7 channels (~150 ms) (Cummins *et al.* 1998; Herzog *et al.* 2003). It could therefore be predicted that Na_v1.2 would respond in a similar way to Na_v1.6 and activate in response to large depolarizations rather than small, slow ones.

Resurgent current was first described in Purkinje neurones and was attributed to the presence of Na_v1.6 in these cells because the current was minimal (~10% of normal) in Na_v1.6-null (med) mice (Raman & Bean, 1997). The current can be inhibited by phosphorylation blockers (Grieco *et al.* 2002) and has been associated with rapid burst firing in response to large depolarizations (Raman *et al.* 1997; Khaliq *et al.* 2003; Swensen & Bean, 2003). More recent studies have led to recognition that other sodium channel isoforms may be able to produce resurgent current as well. The suggestion that this current is produced by an endogenous open-channel blocker is supported by the demonstration of re-emergence of robust resurgent current in Na_v1.6-null Purkinje neurones, when inactivation of the transient current was

slowed (Grieco & Raman, 2004). Further evidence was provided by recordings of the current in subthalamic nuclei (Do & Bean, 2004) and in granule cells, unipolar brush cells and cerebellar nuclei (Afshari *et al.* 2004), although in the latter study, specific recording conditions were manipulated to observe the currents. Grieco *et al.* (2005) provided evidence which supports a role of the cytosolic tail of the sodium channel $\beta 4$ subunit (Yu *et al.* 2003), as the open channel blocker. The evidence for a resurgent current in spinal neurones is less well documented, with studies showing either no occurrence (Pan & Beam, 1999) or its presence only in a subpopulation of large DRG neurones (Cummins *et al.* 2003). Our present work demonstrates that $\text{Na}_v1.6_R$ can produce resurgent current in around 20% of transfected small DRG neurones, and that this current activates over a potential range similar to that found previously in Purkinje neurones (Raman & Bean, 1997). When either $\text{Na}_v1.4$ or $\text{Na}_v1.7$ were expressed in DRG neurones, no resurgent current could be detected in any cells (Cummins *et al.* 2003). In contrast, we show here that $\text{Na}_v1.2_R$ can produce resurgent current in a small number of neurones. The data reported in this study may underestimate the occurrence of $\text{Na}_v1.2_R$ resurgent current because of the smaller size of the transient currents in these cells, since this made detection of the resurgent current much more difficult. Our study confirms that another isoform, in addition to $\text{Na}_v1.6$, is capable of producing a resurgent current within some cells in at least one neuronal background. We suggest that $\text{Na}_v1.2$ could be the sodium channel subtype that gives rise to resurgent current in neurones that do not express $\text{Na}_v1.6$ (Afshari *et al.* 2004; Do & Bean, 2004).

The recovery from inactivation experiments in our study showed that $\text{Na}_v1.2_R$ and $\text{Na}_v1.6_R$ had fast time constants for recovery from a single stimulus and, if anything, $\text{Na}_v1.2_R$ reprimed faster under those test conditions, using a holding potential of -100 mV. However, $\text{Na}_v1.6$ has been associated with rapid, burst firing (Raman *et al.* 1997; Swensen & Bean, 2003) and we therefore examined the response of the currents to trains of stimulation, from a holding potential of -80 mV, to more closely mimic a possible *in vivo* situation. Our data demonstrate that both channels can follow repetitive stimulation up to around 10 Hz. However, at higher frequencies of 20 and 100 Hz, $\text{Na}_v1.6$ currents were able to maintain a more robust transient current, from this holding potential, which may influence other biophysical parameters of the channels, such as slow inactivation. This implies that $\text{Na}_v1.6$ may be able to follow high-frequency trains more faithfully than $\text{Na}_v1.2$. The greater amount of persistent current produced by the $\text{Na}_v1.6$ channel could be, in part, responsible for the ability to follow high frequencies. A recent paper also compared these channels using trains of stimulation, using an oocyte expression system (Zhou & Goldin, 2004). The authors describe a

use-dependent potentiation of the $\text{Na}_v1.6$ channel with high-frequency trains, although a potentiation of endogenous sodium currents in mammalian cells has not been reported in the literature, and we found no evidence for potentiation in the current study.

Conclusions

In this paper, we have studied two sodium channel subtypes expressed in mammalian, neuronal cells and have shown that there are several important differences in their properties. The $\text{Na}_v1.2$ channel may provide a basis for the firing of action potentials, even with strong depolarization, although the kinetics of $\text{Na}_v1.2$ may be best suited to low frequencies of opening. Because $\text{Na}_v1.2$ produces only a small persistent current, selective expression of this channel in some demyelinated axons may provide a basis for maintaining firing capability, at least at lower frequencies, while limiting the sustained Na^+ influx that has been shown (Stys *et al.* 1992) to drive damaging reverse $\text{Na}^+/\text{Ca}^{2+}$ exchange. In contrast, $\text{Na}_v1.6$ expression may allow neurones to fire at high frequencies. However, the larger persistent current produced by $\text{Na}_v1.6$ may play a role in a damaging injury cascade, when coexpressed with the $\text{Na}^+/\text{Ca}^{2+}$ exchanger in demyelinated axons (Craner *et al.* 2004a,b).

References

- Afshari FS, Ptak K, Khaliq ZM, Grieco TM, Slater NT, McCrimmon DR & Raman IM (2004). Resurgent Na currents in four classes of neurons of the cerebellum. *J Neurophysiol* **92**, 2831–2843.
- Akopian AN, Souslova V, England S, Okuse K, Ogata N, Ure J, Smith A, Kerr BJ, McMahon SB, Boyce S, Hill R, Stanfa LC, Dickenson AH & Wood JN (1999). The tetrodotoxin-resistant sodium channel SNS has a specialized function in pain pathways. *Nat Neurosci* **2**, 541–548.
- Baker MD & Bostock H (1997). Low-threshold, persistent sodium current in rat large dorsal root ganglion neurons in culture. *J Neurophysiol* **77**, 1503–1513.
- Black JA, Dib-Hajj S, McNabola K, Jeste S, Rizzo MA, Kocsis JD & Waxman SG (1996). Spinal sensory neurons express multiple sodium channel alpha-subunit mRNAs. *Mol Brain Res* **43**, 117–131.
- Black JA, Renganathan M & Waxman SG (2002). Sodium channel $\text{Na}_v1.6$ is expressed along nonmyelinated axons and it contributes to conduction. *Mol Brain Res* **105**, 19–28.
- Boiko T, Rasband MN, Levinson SR, Caldwell JH, Mandel G, Trimmer JS & Matthews G (2001). Compact myelin dictates the differential targeting of two sodium channel isoforms in the same axon. *Neuron* **30**, 91–104.
- Burbidge SA, Dale TJ, Powell AJ, Whitaker WR, Xie XM, Romanos MA & Clare JJ (2002). Molecular cloning, distribution and functional analysis of the $\text{Na}_v1.6$. Voltage-gated sodium channel from human brain. *Mol Brain Res* **103**, 80–90.

- Caffrey JM, Eng DL, Black JA, Waxman SG & Kocsis JD (1992). Three types of sodium channels in adult rat dorsal root ganglion neurons. *Brain Res* **592**, 283–297.
- Chahine M, George AL Jr, Zhou M, Ji S, Sun W, Barchi RL & Horn R (1994). Sodium channel mutations in paramyotonia congenita uncouple inactivation from activation. *Neuron* **12**, 281–294.
- Craner MJ, Hains BC, Lo AC, Black JA & Waxman SG (2004a). Co-localization of sodium channel $\text{Na}_v1.6$ and the sodium–calcium exchanger at sites of axonal injury in the spinal cord in EAE. *Brain* **127**, 294–303.
- Craner MJ, Lo AC, Black JA & Waxman SG (2003). Abnormal sodium channel distribution in optic nerve axons in a model of inflammatory demyelination. *Brain* **126**, 1552–1561.
- Craner MJ, Newcombe J, Black JA, Hartle C, Cuzner ML & Waxman SG (2004b). Molecular changes in neurons in multiple sclerosis: altered axonal expression of $\text{Na}_v1.2$ and $\text{Na}_v1.6$ sodium channels and $\text{Na}^+/\text{Ca}^{2+}$ exchanger. *Proc Natl Acad Sci U S A* **101**, 8168–8173.
- Cummins TR, Aglieco F, Renganathan M, Herzog RI, Dib-Hajj SD & Waxman SG (2001). $\text{Na}_v1.3$ sodium channels: rapid repriming and slow closed-state inactivation display quantitative differences after expression in a mammalian cell line and in spinal sensory neurons. *J Neurosci* **21**, 5952–5961.
- Cummins TR, Dib-Hajj SD, Black JA, Akopian AN, Wood JN & Waxman SG (1999). A novel persistent tetrodotoxin-resistant sodium current in SNS-null and wild-type small primary sensory neurons. *J Neurosci* **19**, RC43.
- Cummins TR, Dib-Hajj SD, Herzog RI & Waxman SG (2003). $\text{Na}_v1.6$ sodium channels generate resurgent current in primary sensory neurons. *Program No. 8.7 2003 Abstract Viewer/Itinerary Planner*. Society for Neuroscience, Washington, DC.
- Cummins TR, Howe JR & Waxman SG (1998). Slow closed-state inactivation: a novel mechanism underlying ramp currents in cells expressing the hNE/PN1 sodium channel. *J Neurosci* **18**, 9607–9619.
- Cummins TR & Waxman SG (1997). Downregulation of tetrodotoxin-resistant sodium currents and upregulation of a rapidly repriming tetrodotoxin-sensitive sodium current in small spinal sensory neurons after nerve injury. *J Neurosci* **17**, 3503–3514.
- Do MT & Bean BP (2004). Sodium currents in subthalamic nucleus neurons from $\text{Na}_v1.6$ -null mice. *J Neurophysiol* **92**, 726–733.
- Elliott AA & Elliott JR (1993). Characterization of TTX-sensitive and TTX-resistant sodium currents in small cells from adult rat dorsal root ganglia. *J Physiol* **463**, 39–56.
- Everill B, Cummins TR, Waxman SG & Kocsis JD (2001). Sodium currents of large (A beta-type) adult cutaneous afferent dorsal root ganglion neurons display rapid recovery from inactivation before and after axotomy. *Neuroscience* **106**, 161–169.
- Goldin AL, Barchi RL, Caldwell JH, Hofmann F, Howe JR, Hunter JC, Kallen RG, Mandel G, Meisler MH, Netter YB, Noda M, Tamkun MM, Waxman SG, Wood JN & Catterall WA (2000). Nomenclature of voltage-gated sodium channels. *Neuron* **28**, 365–368.
- Grieco TM, Afshari FS & Raman IM (2002). A role for phosphorylation in the maintenance of resurgent sodium current in cerebellar purkinje neurons. *J Neurosci* **22**, 3100–3107.
- Grieco TM, Malhotra JD, Chen C, Isom LL & Raman IM (2005). Open-channel block by the cytoplasmic tail of sodium channel $\beta 4$ as a mechanism for resurgent sodium current. *Neuron* **45**, 233–244.
- Grieco TM & Raman IM (2004). Production of resurgent current in $\text{Na}_v1.6$ -null Purkinje neurons by slowing sodium channel inactivation with β -pompilidotoxin. *J Neurosci* **24**, 35–42.
- Herzog RI, Cummins TR, Ghassemi F, Dib-Hajj SD & Waxman SG (2003). Distinct repriming and closed-state inactivation kinetics of $\text{Na}_v1.6$ and $\text{Na}_v1.7$ sodium channels in mouse spinal sensory neurons. *J Physiol* **551**, 741–750.
- Isom LL, De Jongh KS & Catterall WA (1994). Auxiliary subunits of voltage-gated ion channels. *Neuron* **12**, 1183–1194.
- Kaplan MR, Cho M, Ullian EM, Isom LL, Levinson SR & Barres BA (2001). Differential control of clustering of the sodium channels $\text{Na}_v1.2$ and $\text{Na}_v1.6$ at developing CNS nodes of Ranvier. *Neuron* **30**, 105–119.
- Kearney JA, Plummer NW, Smith MR, Kapur J, Cummins TR, Waxman SG, Goldin AL & Meisler MH (2001). A gain-of-function mutation in the sodium channel gene *Scn2a* results in seizures and behavioral abnormalities. *Neuroscience* **102**, 307–317.
- Khaliq ZM, Gouwens NW & Raman IM (2003). The contribution of resurgent sodium current to high-frequency firing in Purkinje neurons: an experimental and modeling study. *J Neurosci* **23**, 4899–4912.
- Klugbauer N, Lacinova L, Flockerzi V & Hofmann F (1995). Structure and functional expression of a new member of the tetrodotoxin-sensitive voltage-activated sodium channel family from human neuroendocrine cells. *EMBO J* **14**, 1084–1090.
- Ma JY, Catterall WA & Scheuer T (1997). Persistent sodium currents through brain sodium channels induced by G protein $\beta\gamma$ subunits. *Neuron* **19**, 443–452.
- O’Leary ME (1998). Characterization of the isoform-specific differences in the gating of neuronal and muscle sodium channels. *Can J Physiol Pharmacol* **76**, 1041–1050.
- Pan F & Bean KG (1999). The absence of resurgent sodium current in mouse spinal neurons. *Brain Res* **849**, 162–168.
- Raman IM & Bean BP (1997). Resurgent sodium current and action potential formation in dissociated cerebellar purkinje neurons. *J Neurosci* **17**, 4517–4526.
- Raman IM, Sprunger LK, Meisler MH & Bean BP (1997). Altered subthreshold sodium currents and disrupted firing patterns in Purkinje neurons of *Scn8a* mutant mice. *Neuron* **19**, 881–891.
- Rush AM, Brau ME, Elliott AA & Elliott JR (1998). Electrophysiological properties of sodium current subtypes in small cells from adult rat dorsal root ganglia. *J Physiol* **511**, 771–789.
- Smith MR, Smith RD, Plummer NW, Meisler MH & Goldin AL (1998). Functional analysis of the mouse *Scn8a* sodium channel. *J Neurosci* **18**, 6093–6102.

- Stys PK, Sontheimer H, Ransom BR & Waxman SG (1993). Noninactivating, tetrodotoxin-sensitive Na⁺ conductance in rat optic nerve axons. *Proc Natl Acad Sci U S A* **90**, 6976–6980.
- Stys PK, Waxman SG & Ransom BR (1992). Ionic mechanisms of anoxic injury in mammalian CNS white matter: role of Na⁺ channels and Na⁺–Ca²⁺ exchanger. *J Neurosci* **12**, 430–439.
- Swensen AM & Bean BP (2003). Ionic mechanisms of burst firing in dissociated Purkinje neurons. *J Neurosci* **23**, 9650–9663.
- Waxman SG, Davis PK, Black JA & Ransom BR (1990). Anoxic injury of mammalian central white matter: decreased susceptibility in myelin-deficient optic nerve. *Ann Neurol* **28**, 335–340.
- Wellmann H, Kaltschmidt B & Kaltschmidt C (1999). Optimized protocol for biolistic transfection of brain slices and dissociated cultured neurons with a hand-held gene gun. *J Neurosci Meth* **92**, 55–64.
- Westenbroek RE, Merrick DK & Catterall WA (1989). Differential subcellular localization of the RI and RII Na⁺ channel subtypes in central neurons. *Neuron* **3**, 695–704.
- Xie X, Dale TJ, John VH, Cater HL, Peakman TC & Clare JJ (2001). Electrophysiological and pharmacological properties of the human brain type IIA Na⁺ channel expressed in a stable mammalian cell line. *Pflugers Arch* **441**, 425–433.
- Yu FH, Westenbroek RE, Silos-Santiago I, McCormick KA, Lawson D, Ge P, Ferreira H, Lilly J, DiStefano PS, Catterall WA, Scheuer T & Curtis R (2003). Sodium channel β 4, a new disulfide-linked auxiliary subunit with similarity to β 2. *J Neurosci* **23**, 7577–7585.
- Zhou W & Goldin AL (2004). Use-dependent potentiation of the Na_v1.6 sodium channel. *Biophys J* **87**, 3862–3872.

Acknowledgements

We thank Youping Zhang, Shujun Liu, Lynda Tyrell, Pam Zwinger and Bart Toftness for technical assistance; Professor J. N. Wood for the generous gift of the Na_v1.8-null mouse and Professor A. L. Goldin for generously providing the Na_v1.2 and Na_v1.6 plasmids. This work was supported in part by grants from the National Multiple Sclerosis Society; Veterans Administration Rehabilitation Research and Development Service and the Nancy Davis Foundation. The Center for Neuroscience and Regeneration Research is a collaboration of the Paralyzed Veterans of America and the United Spinal Association with Yale University.